

Geometry-Enabled Radiation from Structured Paraxial Electrons

M.S. Epov, I.E. Shenderovich, and S.S. Baturin*

School of Physics and Engineering, ITMO University, St. Petersburg, Russia 197101

(Dated: February 10, 2026)

We present a microscopic calculation of spontaneous photon emission by twisted (paraxial) electrons propagating through inhomogeneous, axisymmetric magnetic fields. We construct exact electron states that incorporate transverse mode structure and wavefront curvature by combining the Foldy-Wouthuysen transformation with a geometric framework based on Lewis-Ermakov invariants and metaplectic transformations. We show that the evolution of such structured states corresponds to an open path in the space of quadratic forms, giving rise to a geometric contribution to the emission amplitude that cannot be eliminated by gauge choice or adiabatic arguments. The inverse radius of curvature of the electron wavefront emerges as an effective geometric field that enables radiation even in regions where the external magnetic field vanishes locally. This mechanism generalizes Landau-level radiation to nonasymptotic, structured electron states and establishes a direct connection between noncyclic geometric evolution and photon emission.

Recent theoretical and experimental studies have established that free electrons, as well as electrons propagating in static magnetic fields, may carry a well-defined projection of orbital angular momentum (OAM) [1–4]. These so-called twisted electron states exhibit nontrivial transverse structure and phase singularities, leading to a range of novel quantum and dynamical effects. Their fundamental properties have been extensively explored [5–14], yet several open questions remain, including the stability of vortex states and their behavior under realistic external-field configurations [2].

Quantum electrodynamical processes involving structured particles—most notably electrons prepared in Laguerre-Gaussian-type modes [15]—have primarily been studied for stationary states and uniform external fields [16], often within the dipole approximation. In such settings, photon emission is conventionally attributed to local acceleration induced by external forces. However, this picture becomes incomplete for nonasymptotic, structured wave packets whose evolution is governed by geometric phases and intrinsic wavefront curvature.

In this work, we develop a theoretical framework for spontaneous photon emission by twisted electrons propagating in a general inhomogeneous axisymmetric magnetic field. Starting from a relativistic description, we apply the Foldy-Wouthuysen transformation [17] followed by a controlled paraxial reduction, which allows the longitudinal coordinate to play the role of an effective evolution parameter. The resulting transverse dynamics is governed by a Lewis-type system with a spatially dependent frequency. By exploiting the Lewis-Riesenfeld invariant theory [18–20] and the Ermakov transformation [21–26], we obtain an exact representation of the electron states in terms of metaplectic transformations acting on harmonic-oscillator eigenstates. This construction provides a nonperturbative and fully geometric de-

scription of twisted electron beams in inhomogeneous magnetic fields.

Our central result is the identification of an irremovable geometric contribution to the photon emission amplitude associated with the inverse radius of curvature of the electron wavefront. This contribution originates from a quadratic phase generated by the metaplectic shear inherent to paraxial evolution and is uniquely fixed by the Ermakov equation. Unlike conventional gauge potentials, this geometric field cannot be eliminated by a gauge transformation without destroying the Lewis invariants and the underlying symplectic structure. As a consequence, photon emission can persist in spatial regions where the external magnetic field locally vanishes, provided the electron wave packet retains finite curvature inherited from its prior evolution in the field. The resulting emission process is intrinsically nonlocal and history dependent: the transition probability is governed by the accumulated geometric phase rather than by the instantaneous local field strength (see Fig. 1). In this respect, the effect is directly analogous to the Aharonov-Bohm

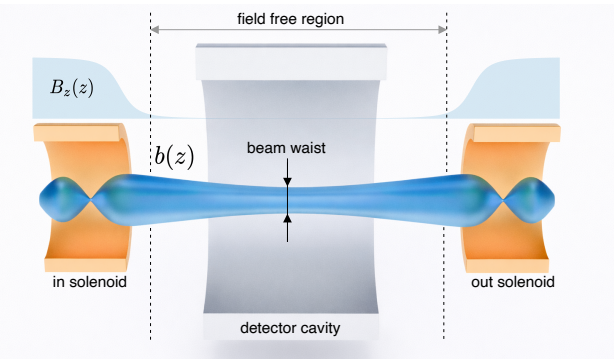


Figure 1. Schematic setup: two solenoids shape an axisymmetric guiding field $B_z(z)$ and imprint a nontrivial Ermakov scaling $b(z)$ (state transverse size and wavefront curvature) on the paraxial twisted-electron mode. Photon detection occurs in the central cavity located in a locally field-free region, where radiation persists due to the inherited curvature.

* s.s.baturin@gmail.com

phenomenon [27], where observable consequences arise from geometric phases encoded in the global structure of the wavefunction rather than from local forces acting along the trajectory.

More broadly, our results generalize radiation mechanisms associated with Landau-level transitions to structured, nonasymptotic electron states and establish a direct connection between geometric dressing of matter waves, photon emission, and concepts familiar from cavity QED [28], where squeezing-induced geometric phases are known to modify light-matter coupling strengths.

Throughout this paper, we adopt natural units with $\hbar = c = 1$ and assume $e < 0$ for the electron charge.

The quantum-mechanical description of relativistic electrons in external electromagnetic fields exhibits a structure closely related to its nonrelativistic counterpart. The dynamics of a relativistic electron in a stationary magnetic field are governed by the Dirac equation [29]

$$(\alpha \hat{\pi} + \beta m) \Psi = i \partial_t \Psi, \quad (1)$$

where $\hat{\pi} = \hat{\mathbf{p}} + |e| \mathbf{A}_{cl}$ is the kinetic momentum operator and $\Psi(\vec{r}, t) = \Psi_{st}(\vec{r}) e^{-iEt}$ is a bispinor with fixed energy E .

We consider an axisymmetric magnetic field predominantly aligned along the z direction,

$$\mathbf{B}(z)^T = [-x B'_z(z)/2, -y B'_z(z)/2, B_z(z)]. \quad (2)$$

The transverse magnetic components are uniquely fixed by the solenoidal condition $\nabla \cdot \mathbf{B} = 0$ and therefore cannot be neglected. In the Coulomb gauge, the corresponding vector potential reads [25]

$$\mathbf{A}_{cl}^T = [-y B_z(z)/2, x B_z(z)/2, 0], \quad (3)$$

which automatically incorporates the transverse magnetic field. Alternative gauge choices redistribute longitudinal and transverse couplings but do not modify the underlying paraxial dynamics (see Ref. [26]).

Applying the Foldy-Wouthuysen transformation and squaring the Hamiltonian yields a Pauli-type equation for the upper spinor Φ_{FW} ,

$$(\hat{\pi}^2 - e \mathbf{B} \cdot \boldsymbol{\sigma}) \Phi_{FW} = k^2 \Phi_{FW}, \quad k^2 = E^2 - m^2. \quad (4)$$

The second term represents the Pauli spin-field interaction. In the regime $||\hat{\pi}_\perp^2|| \gg ||e \mathbf{B} \cdot \boldsymbol{\sigma}||$, the spin interaction energy is parametrically smaller than the kinetic energy, and the electron can be treated to a good approximation as a scalar particle in a magnetic field. In the following, we neglect spin-related effects.

In the paraxial regime $p_z \gg p_\perp$, we write $\Phi_{FW}(\vec{r}, t) = (\psi(\vec{r}), 0)^T \exp(ikz - iEt)$, where the envelope ψ varies slowly along z . This leads to the scalar paraxial equation

$$\hat{\pi}_\perp^2 \psi = 2ik \partial_z \psi, \quad (5)$$

which has the form of a Schrödinger equation with the propagation coordinate z playing the role of time.

Expanding the kinetic momentum operator, Eq. (5) can be rewritten as

$$i \frac{\partial \psi}{\partial z} = [\hat{\mathcal{H}}_\perp(z) + \Omega(z) \hat{L}_z] \psi, \quad (6)$$

$$\hat{\mathcal{H}}_\perp(z) = \frac{\hat{p}_\perp^2}{2} + \frac{\Omega^2(z) \hat{\rho}^2}{2}, \quad (7)$$

where \hat{L}_z is the orbital angular momentum operator and $\hat{\rho}^2 = \hat{x}^2 + \hat{y}^2$. We introduce normalized coordinates $\tilde{z} = z/(k\rho_H^2)$, $\tilde{x} = x/\rho_H$, and $\tilde{y} = y/\rho_H$, where the magnetic length and normalized frequency are defined as

$$\rho_H = \sqrt{\frac{2}{|e| \max |B_z(z)|}}, \quad \Omega(z) = \frac{B_z(z)}{\max |B_z(z)|}. \quad (8)$$

For clarity, we drop tildes in the following and work exclusively with normalized variables.

The Larmor rotation operator

$$\hat{R} = \exp \left[-i \int_0^z d\tilde{z} \Omega(\tilde{z}) \hat{L}_z \right] \quad (9)$$

can be factored out exactly, since $\hat{\mathcal{H}}_\perp(z)$ commutes with $\Omega(z) \hat{L}_z$ for all z . This commutation follows directly from the rotational symmetry of the transverse harmonic confinement. The remaining dynamics generated by $\hat{\mathcal{H}}_\perp(z)$ together with $i\partial_z$ constitutes a Lewis-type system: a two-dimensional harmonic oscillator with z -dependent frequency, where the propagation coordinate z replaces time.

This two-dimensional system decomposes into two equivalent one-dimensional subsystems, each admitting an exact invariant of motion,

$$\hat{I}_x = \frac{(b\hat{p}_x - b'x)^2}{2} + \frac{\hat{x}^2}{2b^2}, \quad (10)$$

$$\hat{I}_y = \frac{(b\hat{p}_y - b'y)^2}{2} + \frac{\hat{y}^2}{2b^2}. \quad (11)$$

Here $b(z)$ satisfies the Ermakov equation

$$b'' + \Omega^2(z)b = \frac{1}{b^3}, \quad b(0) = b_0, \quad b'(0) = b'_0. \quad (12)$$

The Ermakov function $b(z)$ is uniquely fixed by the field profile $\Omega(z)$ and the initial conditions.

The invariants (10) are unitarily equivalent to the Hamiltonian of a unit-frequency harmonic oscillator via a composition of metaplectic transformations,

$$\hat{H}_0 = \hat{S}^\dagger \hat{M}^\dagger (\hat{I}_x + \hat{I}_y) \hat{M} \hat{S}, \quad (13)$$

where

$$\hat{H}_0 = \frac{\hat{p}_\perp^2}{2} + \frac{\hat{\rho}^2}{2}, \quad (14)$$

$$\hat{S} = \exp \left[-i \frac{\ln b}{2} (\hat{\rho} \cdot \hat{\mathbf{p}}_\perp + \hat{\mathbf{p}}_\perp \cdot \hat{\rho}) \right], \quad (15)$$

$$\hat{M} = \exp \left[i \frac{b'}{b} \frac{\hat{\rho}^2}{2} \right]. \quad (16)$$

The Lewis-Ermakov invariants thus serve a dual role: they label the transverse modes and simultaneously encode the canonical transformation that renders the z -dependent dynamics stationary. Indeed, the structure of $\hat{I}_{x,y}$ suggests introducing new phase-space variables $(\hat{Q}_{x,y}, \hat{P}_{x,y})$ defined by $Q_j = x_j/b$ and $P_j = b\hat{p}_j - b'x_j$, in terms of which each invariant takes the standard harmonic-oscillator form $\hat{I}_j = \frac{1}{2}(\hat{P}_j^2 + \hat{Q}_j^2)$. The operators \hat{S} and \hat{M} implement the corresponding symplectic transformation at the quantum level, providing its metaplectic lift [30].

The full solution of Eq. (6) can therefore be written as a squeezed coherent state (for the relevant derivations see Ref.[31])

$$\psi = \hat{R}\hat{U}\hat{M}\hat{S}|n_+, n_-\rangle, \quad (17)$$

where $|n_+, n_-\rangle$ is a fixed Fock state of the two-dimensional harmonic oscillator and n_+ and n_- are the left and right circular numbers. In the polar configuration space the state has the form of a Laguerre-Gaussian (twisted) mode [32]

$$\begin{aligned} \langle \rho, \varphi | n_+, n_- \rangle &= & (18) \\ &\sqrt{\frac{n_r!}{\pi(n_r + |l|)!}} \rho^{|l|} \exp\left(-\frac{\rho^2}{2}\right) \mathcal{L}_{n_r}^{|l|}(\rho^2) \exp(il\varphi), \\ n_r &= \min(n_+, n_-), \quad l = n_+ - n_- \end{aligned}$$

Above \mathcal{L} is the generalized Laguerre polynomial and we imply standard normalization for the generalized ladder operators

$$\hat{a}_\pm = \frac{\hat{a}_x \mp i\hat{a}_y}{\sqrt{2}}, \quad [\hat{a}_\pm, \hat{a}_\pm^\dagger] = 1. \quad (19)$$

The operator

$$\hat{U} = \exp\left[-i(n_+ + n_- + 1) \int_0^z \frac{d\bar{z}}{b^2(\bar{z})}\right] \quad (20)$$

contains the Lewis phase accumulated along the propagation.

Geometrically, the Lewis phase represents the holonomy of the connection induced by the metaplectic representation on the bundle of invariant eigenstates. For cyclic evolution it reduces to a purely geometric phase determined by the enclosed curvature, while for open trajectories relevant to realistic structured electron beams it acquires boundary contributions that cannot be removed by gauge choice. Unlike a conventional gauge phase, this quadratic (metaplectic) phase is fixed once the Lewis-Ermakov invariant structure and boundary conditions are specified; it cannot be removed by a rephasing that preserves the invariant eigenbasis and the associated symplectic (metaplectic) map. It represents the geometric dressing of the electron wavefunction by the external magnetic field, encoding the cumulative effect of transverse focusing into a history-dependent phase. Physically, this implies that the electron propagates not as a

free particle, but as a “dressed” mode that dynamically adapts its wavefront curvature to the profile of the guiding magnetic potential.

Finally, we emphasize that the ordering of the metaplectic operators in Eq. (17) is fixed by the structure of the invariants (10).

Now we focus on the spontaneous emission process $e_i \rightarrow e_f + \gamma$ for a relativistic twisted electron propagating along the z -axis in an inhomogeneous magnetic field. The theoretical framework is based on scalar QED, where the photon is a plane-wave mode and the electron wavefunction is given by a paraxial state in a non-uniform magnetic field given by

$$\Psi = \frac{1}{\sqrt{L}} \psi \exp[i\chi^2 z - iEt]. \quad (21)$$

where the transverse part ψ is defined in Eq.(17), k as before the total wave vector of the electron, E is the total energy and L is the finite z -length of the considered volume measured in the units of $k\rho_H^2$ and

$$\chi = k\rho_H. \quad (22)$$

The first-order transition amplitude is [33]

$$S_{fi} = i \int_{-\infty}^{\infty} dt \int_{-\infty}^{\infty} dx \int_{-\infty}^{\infty} dy \int_{-L/2}^{L/2} dz \mathbf{j}_{fi} \cdot \mathbf{A}_{ph}, \quad (23)$$

$$\mathbf{j}_{fi} = \frac{e\beta}{2\chi} [\Psi_f^* (\hat{\pi} \Psi_i) + \Psi_i (\hat{\pi} \Psi_f)^*] \quad (24)$$

where $\mathbf{A}_{ph} = \frac{\epsilon}{\sqrt{2\omega V}} \exp(-i\omega t) \exp(i\rho_H \mathbf{k}_\perp^\omega \cdot \boldsymbol{\rho} + ik\rho_H^2 k_z^\omega z)$ is the photon wave function with the photon wave vector $\mathbf{k}^\omega = \omega(\sin\theta \cos\varphi, \sin\theta \sin\varphi, \cos\theta)^T$ and polarization vector ϵ satisfying the transversality condition $\epsilon^* \cdot \mathbf{k}^\omega = 0$ and $\beta = k/E$ is the electron relativistic beta-factor.

We note that as before all spatial coordinates are dimensionless, the kinetic momentum operator is dimensionless as well and normalized to $1/\rho_H$. We integrate over the time and get

$$\begin{aligned} S_{fi} &= \int_{-L/2}^{L/2} dz \frac{\pi ie\beta}{\chi L \sqrt{2\omega V}} \delta(E_f + \omega - E_i) \times & (25) \\ &\quad \epsilon^* \cdot \left[\int \Psi_f^* \{ \exp(-i\boldsymbol{\kappa} \cdot \hat{\mathbf{r}}) \hat{\pi} \}_+ \Psi_i dx dy \right]. \end{aligned}$$

Above $\boldsymbol{\kappa} = \rho_H(k_x^\omega, k_y^\omega, \chi k_z^\omega)^T$, $\{\cdot, \cdot\}_+$ is the anticommutator and $\hat{\pi} = (\hat{p}_x - \Omega(z)\hat{y}, \hat{p}_y + \Omega(z)x, \hat{p}_z/\chi)^T$ We note that

$$\{\exp(-i\boldsymbol{\kappa} \cdot \hat{\mathbf{r}}), \hat{\pi}\}_+ = \exp(-i\boldsymbol{\kappa} \cdot \hat{\mathbf{r}}) [2\hat{\pi} - \rho_H \mathbf{k}^\omega] \quad (26)$$

switch to the Fock representation, and rewrite Eq.(25) in a slightly modified form

$$\begin{aligned} S_{fi} &= & (27) \\ &\int_{-L/2}^{L/2} \frac{2\pi ie\beta}{\chi L \sqrt{2\omega V}} [s_\perp(z) + s_\parallel(z)] \delta(E_f + \omega - E_i) dz. \end{aligned}$$

with

$$s_{\perp}(z) = \exp[i\delta\phi(z)] \times \langle n_+^f, n_-^f | \hat{S}^\dagger \hat{M}^\dagger \boldsymbol{\epsilon}_{\perp}^* \cdot \hat{\mathbf{J}}_{\perp} \hat{M} \hat{S} | n_+^i, n_-^i \rangle. \quad (28)$$

Above the operator $\hat{\mathbf{J}}_{\perp}$ is given by

$$\hat{\mathbf{J}}_{\perp} = \exp(-i\boldsymbol{\kappa}_{\perp} \cdot \hat{\boldsymbol{\rho}}) \hat{\boldsymbol{\pi}}_{\perp}. \quad (29)$$

The function $s_{\parallel}(z)$ in the second term of the Eq.(27) is given by

$$s_{\parallel}(z) = \frac{\exp[i\delta\phi(z)]}{\chi} \langle n_+^f, n_-^f | \hat{S}^\dagger \hat{M}^\dagger \boldsymbol{\epsilon}_z^* \hat{\mathbf{J}}_z \hat{M} \hat{S} | n_+^i, n_-^i \rangle, \quad (30)$$

with

$$\hat{\mathbf{J}}_z = \exp(-i\boldsymbol{\kappa}_{\perp} \cdot \hat{\boldsymbol{\rho}}) [\hat{\mathcal{H}}_{\perp}(z) + \Omega(z) \hat{L}_z]. \quad (31)$$

Above $\hat{\mathcal{H}}_{\perp}(z)$ is given by Eq.(7) and we have used the identity between the right and the left hand side of Eq.(6). The common phase factor is given by

$$\begin{aligned} \delta\phi(z) &= \frac{\Delta k - k_z^{\omega}}{k^i} \chi^2 z - \Delta N \int_{-L/2}^z \frac{d\bar{z}}{b^2(\bar{z})} - \Delta l \int_{-L/2}^z \Omega(\bar{z}) d\bar{z}. \\ \Delta N &= \Delta n_+ + \Delta n_-, \quad \Delta l = \Delta n_+ - \Delta n_-, \\ \Delta k &= k^i - k^f, \quad \chi = k^i \rho_H. \end{aligned} \quad (32)$$

For the common laboratory (electron microscope) setup parameter χ is significantly larger than unity. For instance for the peak magnetic field $\max |B(z)| \sim 1$ T of the magnetic guiding system and the electron kinetic energy $W_e \sim 100$ keV we have for the characteristic magnetic length $\rho_H = 36.3$ nm and for the modulus of the electron wave vector $k = 1.7$ pm⁻¹. This results in $\chi \approx 6.2 \times 10^4$. To proceed further we assume χ to be large and neglect the $s_{\parallel}(z)$ contribution to the transition amplitude as it is suppressed by $1/\chi$ factor in comparison to the $s_{\perp}(z)$.

To proceed we first calculate the transformation under the brackets in Eq.(43)

$$\hat{S}^\dagger \hat{M}^\dagger \hat{\mathbf{J}}_{\perp} \hat{M} \hat{S} = \exp[-ib(z)\boldsymbol{\kappa}_{\perp} \cdot \hat{\boldsymbol{\rho}}] \hat{\boldsymbol{\pi}}_{\perp} \quad (33)$$

with

$$\hat{\boldsymbol{\pi}}_{\perp} = \frac{\hat{\mathbf{p}}_{\perp}}{b(z)} + b'(z)\hat{\boldsymbol{\rho}} + b(z)\Omega(z)\mathbf{u}_z \times \hat{\boldsymbol{\rho}} \quad (34)$$

above \mathbf{u}_z is the unit vector along the z -axis. In a locally field-free region, $\Omega(z) = 0$, while the curvature term $b'(z)\hat{\boldsymbol{\rho}}$ remains. This term is fixed by the metaplectic shear (and hence by the Ermakov solution) and therefore acts as an effective geometric driving that enables radiation even when $B_z(z) = 0$ locally.

It is convenient to rewrite operator Eq.(34) in a circular form

$$\hat{\boldsymbol{\pi}}_{\sigma} = \hat{\pi}_x + \sigma i \hat{\pi}_y \quad (35)$$

where $\sigma = \pm$ and denote right and left circular component. Switching to generalized ladder operators we have

$$\hat{\pi}_{-\sigma} = C_{a,\sigma} \hat{a}_{\sigma} + C_{a^{\dagger},\sigma} \hat{a}_{\sigma}^{\dagger}, \quad (36)$$

The coefficients are given by.

$$\begin{aligned} C_{a,\sigma} &= b'(z) - \sigma i b(z) \Omega(z) - \frac{i}{b(z)}, \\ C_{a^{\dagger},\sigma} &= b'(z) - \sigma i b(z) \Omega(z) + \frac{i}{b(z)}. \end{aligned} \quad (37)$$

The exponent in Eq.(33) factorizes as

$$\exp[-ib(z)\boldsymbol{\kappa}_{\perp} \cdot \hat{\boldsymbol{\rho}}] = \prod_{\sigma=\pm} \exp[-i(\kappa_{\sigma} \hat{a}_{\sigma} + \kappa_{\sigma}^* \hat{a}_{\sigma}^{\dagger})], \quad (38)$$

with

$$\kappa_{\sigma} = \frac{b(z)\rho_H k_{\perp}^{\omega}}{2} \exp(\sigma i \varphi). \quad (39)$$

Because the transverse Hamiltonian Eq.(14) is a sum of two commuting 1D oscillators, the Fock space factorizes as $|n_+, n_-\rangle = |n_+\rangle \otimes |n_-\rangle$ with $[\hat{a}_+, \hat{a}_-] = [\hat{a}_+, \hat{a}_-^{\dagger}] = 0$. Given the factorization Eq.(38) we note that matrix element $s_{\perp}(z)$ can be expressed as a product of one dimensional form factors that we define as

$$\begin{aligned} \mathcal{F}_{n_{\sigma}^f, n_{\sigma}^i}(\kappa_{\sigma}) &= \langle n_{\sigma}^f | \hat{D}_{\sigma}(-i\kappa_{\sigma}^*) | n_{\sigma}^i \rangle, \\ \hat{D}_{\sigma}(-i\kappa_{\sigma}^*) &= \exp[-i(\kappa_{\sigma} \hat{a}_{\sigma} + \kappa_{\sigma}^* \hat{a}_{\sigma}^{\dagger})]. \end{aligned} \quad (40)$$

This is a common matrix element of a displacement operator \hat{D}_{σ} that can be evaluated analytically from the action of the ladder operators on the number states. We sketch derivation in the Appendix A and provide the exact expression for $\mathcal{F}_{n_{\sigma}^f, n_{\sigma}^i}(\kappa_{\sigma})$.

With the help of Eq.(35) one may immediately evaluate the weighting coefficient and express it in terms of C functions of Eq.(37) and form factors Eq.(40)

$$\begin{aligned} \mathcal{P}_{n_{\sigma}^f, n_{\sigma}^i}(z) &\equiv \langle n_{\sigma}^f | \hat{D}_{\sigma}(-i\kappa_{\sigma}^*) \hat{\pi}_{-\sigma}(z) | n_{\sigma}^i \rangle = \\ C_{a,\sigma} \sqrt{n_{\sigma}^i} \mathcal{F}_{n_{\sigma}^f, n_{\sigma}^i-1}(\kappa_{\sigma}) &+ C_{a^{\dagger},\sigma} \sqrt{n_{\sigma}^i + 1} \mathcal{F}_{n_{\sigma}^f, n_{\sigma}^i+1}(\kappa_{\sigma}). \end{aligned} \quad (41)$$

We note that above \mathcal{F} and the coefficients $C_{a,\sigma}, C_{a^{\dagger},\sigma}$ depend on $b(z)$, $b'(z)$ and $\Omega(z)$, and thus inherit a parametric z -dependence. Next we use the identity

$$\epsilon_{\lambda, \perp}^* \cdot \hat{\boldsymbol{\pi}}_{\perp} = \frac{1}{2} \sum_{\sigma=\pm} \epsilon_{\lambda\sigma}^* \hat{\pi}_{-\sigma}. \quad (42)$$

with $\lambda = \pm 1$ corresponding to the photon polarization and proceed to the final expression for the $s_{\perp}(z)$ in a compact form

$$s_{\perp}(z) = \frac{e^{i\delta\phi(z)}}{2} \sum_{\sigma=\pm} \epsilon_{\lambda\sigma}^* \mathcal{P}_{n_{\sigma}^f, n_{\sigma}^i} \prod_{\sigma' \neq \sigma} \mathcal{F}_{n_{\sigma'}^f, n_{\sigma'}^i}(\kappa_{\sigma'}). \quad (43)$$

The polarization vector component is given by

$$\epsilon_{\lambda\sigma} = \frac{\cos\theta - \lambda\sigma}{\sqrt{2}} \exp(\sigma i\varphi). \quad (44)$$

Equations (43), (32), and (37) provide the general emission amplitude in an arbitrary axisymmetric inhomogeneous field. The geometry enters through the accumulated Lewis/Larmor phase given by Eq.(32), through the phase of the coefficients $C_{a,\sigma}$, $C_{a^\dagger,\sigma}$ (Eq.(37)) and the displacement parameters κ_σ , all determined by $b(z)$ and $b'(z)$. This dependence in a general case of inhomogeneous magnetic field enables engineered enhancement or suppression of the photon emission.

Next we evaluate the differential emission probability $d\dot{w} = dw/T = |S_{fi}|^2/Tdn_\omega$ in a field-free region $\Omega = 0$. Here $dn_\omega = V\omega^2 \sin\theta d\theta d\varphi/(2\pi)^3$ is the photon density of states in vacuum. With the help of Eq.(27) we get

$$d\dot{w} = \alpha \frac{4\pi\beta^2}{\chi^2 L^2} \frac{2\pi\delta(E_f + \omega - E_i)}{2\omega V} \left| \int_{-L/2}^{L/2} s_\perp(z) dz \right|^2 dn_\omega \quad (45)$$

Above we used the identity $e^2 = 4\pi\alpha$ with α being the fine structure constant. We calculate the integral under the modulus in the dipole approximation (that is well justified by the large $\chi \gg 1$), integrate over ω and φ angle of the photon (see Appendix C for details), sum over the photon polarizations and arrive at the expression for the differential rate for the twisted states with the initial orbital angular momentum ℓ^i

$$\frac{d\dot{w}}{d\theta} = \ell^i \frac{\alpha\beta^4\gamma m_e}{\chi^4} R(\theta, L, b_0). \quad (46)$$

Above the normalized rate that we plot in Fig.2 for relevant parameters is given by

$$R(\theta, L, b_0) = \frac{[\sin X]^4}{X^2} \frac{[1 + (\cos\theta)^2] \sin\theta}{8b_0^4}, \quad (47)$$

$$X = \frac{1 - \beta \cos\theta}{8b_0^2} L.$$

The structure of $R(\theta, L, b_0)$ reveals a characteristic diffractive pattern where the interaction length L acts as an aperture. One may say that this rate describes a boundary effect analogous to Fraunhofer diffraction on a finite slit. Aside from the finite-length interference envelope $[\sin X]^4/X^2$, the rate given by Eq.(46) coincides with the standard electric-dipole (E1) Landau-transition scaling for the channel $n_r = 0$ and $\Delta\ell = +1$. It is proportional to the initial Landau quantum number (i.e., $\propto \ell^i$), carries the usual fine-structure constant factor α , and reproduces the expected paraxial/relativistic dependence through β , γ , and the magnetic-length scale via $\chi = k\rho_H$ (with $\rho_H^2 = 2/(|e|B_{\max})$ and $B_{\max} = \max|B_z(z)|$).

Experimental setup shown in Fig. 1 can be implemented in a transmission electron microscope, where vortex beams are routinely produced [7, 10, 34–37]. For

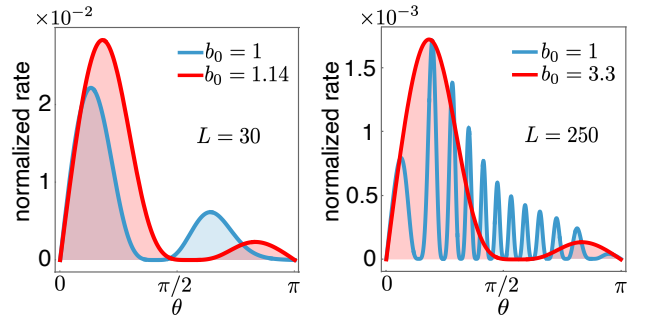


Figure 2. Normalized differential rates for the field-free region calculated for $\beta = 0.548$ (electron kinetic energy 100 keV) using Eq.(47) as a function of the angle θ . The left panel uses interaction length $L = 30$ and the right panel uses $L = 250$ (both in units of $k\rho_H^2$).

$B_{\max} = 1\text{--}10\text{ T}$, $W_e \simeq 100\text{ keV}$, $b_0 = 1.14$, and $L = 30$, Eq. (46) corresponds to microwave emission in the $\nu \simeq 4.5\text{--}45\text{ GHz}$ range and a field-free interaction length of $6.7\text{--}0.67\text{ cm}$. The free-space rate integrated over θ scales as $\ell^i \times (0.25\text{--}2.5)\text{ s}^{-1}$. For the initial orbital angular momentum projection $\ell^i \simeq 10^3$ (as reported in Ref. [38]) and $B_{\max} \simeq 10\text{ T}$ this yields a total count of order $2.5 \times 10^3\text{ s}^{-1}$, compatible with superconducting microwave readout. A resonant cavity can further enhance the detectable count via the Purcell factor [39].

In conclusion, we developed a general QED framework for paraxial structured charged particles in axisymmetric, z -dependent external fields. A key consequence is that these states can radiate in a locally field-free region: the emission amplitude retains a geometric ‘‘memory’’ of the prior evolution through the Ermakov scaling $b(z)$ (and $b'(z)$), and in the appropriate limit the rate recovers Landau-like transition scaling while being governed primarily by the finite-length edges rather than the bulk. The phase cancellation that would suppress emission in an exactly field-free region is fragile, so weak background fields can modify the accumulated phase and may *increase* the net rate. Finally, breathing (nonstationary Landau) structured states [40, 41] in inhomogeneous [24, 26] can be manipulated to enhance or suppress emission by tailoring $b(z)$, providing a geometric control knob for tunable radiation from structured electron beams. Beyond the dipole channel, transitions with $\Delta\ell > 1$ exhibit a saddle-point structure in the emission integral, leading to a preference for higher-order OAM-changing processes. In the paraxial large- χ regime these channels are parametrically suppressed as $\sim 1/\chi$ relative to the dipole contribution; however, when $\chi \sim \mathcal{O}(1)$ they are no longer suppressed and can dominate the dipole rate.

Appendix A: Evaluation of the form factor

It is known that

$$\hat{D}(\alpha) = \exp(\alpha \hat{a}^\dagger - \alpha^* \hat{a}) = e^{-|\alpha|^2/2} e^{\alpha \hat{a}^\dagger} e^{-\alpha^* \hat{a}}. \quad (\text{A1})$$

For the matrix element we write

$$\begin{aligned} \langle n_f | \hat{D}(\alpha) | n_i \rangle &= e^{-|\alpha|^2/2} \langle n_f | e^{\alpha \hat{a}^\dagger} e^{-\alpha^* \hat{a}} | n_i \rangle \\ &= e^{-|\alpha|^2/2} \sum_{k=0}^{\infty} \sum_{m=0}^{\infty} \frac{\alpha^k (-\alpha^*)^m}{k! m!} \langle n_f | (\hat{a}^\dagger)^k \hat{a}^m | n_i \rangle. \end{aligned} \quad (\text{A2})$$

We assume $m \leq n_i$ and use the standard action of the ladder operators

$$\hat{a}^m |n\rangle = \sqrt{\frac{n!}{(n-m)!}} |n-m\rangle, \quad (\text{A3})$$

$$(\hat{a}^\dagger)^k |n\rangle = \sqrt{\frac{(n+k)!}{n!}} |n+k\rangle. \quad (\text{A4})$$

Applying \hat{a}^m first and then $(\hat{a}^\dagger)^k$ yields

$$\langle n_f | (\hat{a}^\dagger)^k \hat{a}^m | n_i \rangle = \frac{\sqrt{n_i! n_f!}}{(n_i - m)!} \delta_{n_f, n_i - m + k}, \quad (\text{A5})$$

where implicitly $m \leq n_i$ (otherwise the term vanishes). We introduce

$$\ell \equiv n_f - n_i > 0, \quad (\text{A6})$$

so that the Kronecker delta enforces $k = \ell + m$. Substituting this constraint into Eq. (A2) and using $\alpha^{\ell+m} (-\alpha^*)^m = \alpha^\ell (-1)^m |\alpha|^{2m}$, we obtain the single finite sum

$$\begin{aligned} \langle n_f | \hat{D}(\alpha) | n_i \rangle &= \\ e^{-|\alpha|^2/2} \alpha^\ell \sqrt{n_i! n_f!} \sum_{m=0}^{n_i} \frac{(-1)^m |\alpha|^{2m}}{m! (\ell+m)! (n_i - m)!} &= \\ e^{-|\alpha|^2/2} \sqrt{\frac{n_i!}{n_f!}} \alpha^\ell \sum_{m=0}^{n_i} (-1)^m \frac{n_f!}{(n_i - m)! (\ell+m)! m!} |\alpha|^{2m}. \end{aligned} \quad (\text{A7})$$

The generalized Laguerre polynomial is defined as

$$\mathcal{L}_n^\ell(x) = \sum_{m=0}^n (-1)^m \frac{(n+\ell)!}{(n-m)! (\ell+m)! m!} x^m. \quad (\text{A8})$$

With $n = n_i$, $\ell = n_f - n_i$, and $(n_i + \ell)! = n_f!$, Eq. (A7) becomes

$$\begin{aligned} \langle n_f | \hat{D}(\alpha) | n_i \rangle &= \\ e^{-|\alpha|^2/2} \sqrt{\frac{n_i!}{n_f!}} \alpha^{n_f - n_i} \mathcal{L}_{n_i}^{n_f - n_i} (|\alpha|^2). \end{aligned} \quad (\text{A9})$$

This is valid for the case $n_f \geq n_i$. In the case $n_i > n_f$, one similarly obtains

$$\begin{aligned} \langle n_f | \hat{D}(\alpha) | n_i \rangle &= \\ e^{-|\alpha|^2/2} \sqrt{\frac{n_f!}{n_i!}} (-\alpha^*)^{n_i - n_f} \mathcal{L}_{n_f}^{n_i - n_f} (|\alpha|^2), \end{aligned} \quad (\text{A10})$$

Finally, using Eqs.(A9) and (A10), we can write the required form factors. For the case of $n_\sigma^f \geq n_\sigma^i$ we have

$$\begin{aligned} \mathcal{F}_{n_\sigma^f, n_\sigma^i}(\kappa_\sigma) &= \\ (-i\kappa_\sigma^*)^{n_\sigma^f - n_\sigma^i} \sqrt{\frac{n_\sigma^i!}{n_\sigma^f!}} \exp\left(-\frac{|\kappa_\sigma|^2}{2}\right) \mathcal{L}_{n_\sigma^i}^{n_\sigma^f - n_\sigma^i} (|\kappa_\sigma|^2), \end{aligned} \quad (\text{A11})$$

and for the case of $n_\sigma^f \leq n_\sigma^i$

$$\begin{aligned} \mathcal{F}_{n_\sigma^f, n_\sigma^i}(\kappa_\sigma) &= \\ (-i\kappa_\sigma)^{n_\sigma^i - n_\sigma^f} \sqrt{\frac{n_\sigma^f!}{n_\sigma^i!}} \exp\left(-\frac{|\kappa_\sigma|^2}{2}\right) \mathcal{L}_{n_\sigma^f}^{n_\sigma^i - n_\sigma^f} (|\kappa_\sigma|^2). \end{aligned} \quad (\text{A12})$$

Appendix B: Photon wave vector

Since the transverse dynamics is governed by a two-dimensional oscillator, $\hat{\pi}_\perp^2$ is proportional to the total transverse excitation number $N = n_+ + n_-$ (in unnormalized units, $\Delta(\hat{\pi}_\perp^2) \propto \Delta N / \rho_H^2$). In the paraxial regime, the energy change is dominated by the change of transverse kinetic energy, thus we get

$$\begin{aligned} \omega(z) &\simeq E_i - E_f \simeq \frac{\Delta(\hat{\pi}_\perp^2)}{2E} = \\ &= \frac{\beta}{2k\rho_H^2} \left[\left(b'^2 + \frac{1}{b^2} + \Omega^2 b^2 \right) \Delta N + 2\Omega\Delta l \right], \end{aligned} \quad (\text{B1})$$

where $\beta = k/E$ is the relativistic β -factor. Thus one obtains

$$\begin{aligned} \left(\frac{k_z^\omega}{k} \right) \chi^2 &\simeq \\ \frac{\beta}{2} \cos \theta \left[\left(b'^2 + \frac{1}{b^2} + \Omega^2 b^2 \right) \Delta N + 2\Omega\Delta l \right]. \end{aligned} \quad (\text{B2})$$

Similarly, one obtains

$$\begin{aligned} \rho_H k_\perp^\omega &\simeq \\ \frac{\beta \sin \theta}{2\chi} \left[\left(b'^2 + \frac{1}{b^2} + \Omega^2 b^2 \right) \Delta N + 2\Omega\Delta l \right]. \end{aligned} \quad (\text{B3})$$

Appendix C: Field-free region

In a field-free region, $\Omega = 0$ and the Ermakov equation reduces to

$$b'' = \frac{1}{b^3}. \quad (\text{C1})$$

With the initial conditions $b'(0) = 0$ and $b(0) = b_0$, we obtain the well-known envelope

$$b(z) = b_0 \sqrt{1 + \frac{z^2}{b_0^4}} \quad (\text{C2})$$

Restoring dimensions via $z = k\rho_H^2 z_{ph}$, we obtain

$$w(z) = w_0 \sqrt{1 + \left(\frac{z_{ph}}{z_R}\right)^2}. \quad (\text{C3})$$

Here $w(z)$ is the state width, $w_0 = \rho_H b_0$ is the state waist, and $z_R = k\rho_H^2 b_0^2$ is the Rayleigh length. We have the following identity

$$b'(z)^2 + \frac{1}{b(z)^2} = \frac{1}{b_0^2}. \quad (\text{C4})$$

Using Eq.(C4), we get

$$\omega \simeq \frac{\beta \Delta N}{2b_0^2 k \rho_H^2} \quad (\text{C5})$$

and

$$\left(\frac{k_z^\omega}{k}\right) \chi^2 \simeq \frac{\beta \Delta N}{2b_0^2} \cos \theta. \quad (\text{C6})$$

as well as

$$\rho_H k_\perp^\omega \simeq \frac{\beta \Delta N \sin \theta}{2\chi b_0^2}. \quad (\text{C7})$$

We neglect recoil and estimate Δk as

$$\frac{\Delta k}{k} \chi^2 \simeq \frac{\Delta N}{2b_0^2} \quad (\text{C8})$$

The C coefficients simplify to

$$\begin{aligned} C_{a,\sigma} &= \frac{1}{b_0} \exp \left[-i \arctan \left(\frac{b_0^2}{z} \right) \right], \\ C_{a^\dagger,\sigma} &= \frac{1}{b_0} \exp \left[i \arctan \left(\frac{b_0^2}{z} \right) \right]. \end{aligned} \quad (\text{C9})$$

The Lewis phase simplifies to

$$\int_0^z \frac{d\bar{z}}{b(\bar{z})^2} = \arctan \left[\frac{z}{b_0^2} \right] \quad (\text{C10})$$

In the dipole case, $\Delta N = N^i - N^f = 1$ (for $\ell^i > 0$), $\Delta \ell = \ell^i - \ell^f = 1$, and for $n_r = 0$ (so that $n_+ = \ell$ and $n_- = 0$) the factor $\mathcal{P}(z)$ is

$$\mathcal{P}_{n_+^f n_+^i}(z) = \frac{1}{b_0} \exp \left[-i \arctan \left(\frac{b_0^2}{z} \right) \right] \sqrt{\ell^i} \quad (\text{C11})$$

With \mathcal{P} given above, we can evaluate the z integral

$$\begin{aligned} \left| \int_{-L/2}^{L/2} s_\perp(\bar{z}) d\bar{z} \right|^2 &= \frac{\ell^i}{b_0^2} \frac{(1 - \lambda \cos \theta)^2}{8} \times \\ &\left| \int_{-L/2}^0 \exp \left[iA\bar{z} + i\frac{\pi}{2} \right] d\bar{z} + \int_0^{L/2} \exp \left[iA\bar{z} - i\frac{\pi}{2} \right] d\bar{z} \right|^2 \\ &= \frac{\ell^i}{b_0^2} \frac{(1 - \lambda \cos \theta)^2}{8} \frac{L^2 [\sin X]^4}{X^2} \end{aligned} \quad (\text{C12})$$

Above

$$A = \frac{1 - \beta \cos \theta}{2b_0^2}, \quad (\text{C13})$$

and

$$X = \frac{1 - \beta \cos \theta}{8b_0^2} L \quad (\text{C14})$$

After integrating over φ and ω , the rate reads

$$d\dot{w} = \alpha \frac{\beta^2}{\chi^2 L^2} \Delta E \sin \theta \left| \int_{-L/2}^{L/2} s_\perp(z) dz \right|^2 d\theta \quad (\text{C15})$$

where ΔE is given by Eq. (C5), since the delta function enforces $\omega = \Delta E$.

After summing over the photon polarizations and simplifying, we obtain

$$\frac{d\dot{w}}{d\theta} = \ell^i \frac{\alpha \beta^4 \gamma m_e}{\chi^4} \frac{[\sin X]^4}{X^2} \frac{[1 + (\cos \theta)^2] \sin \theta}{8b_0^4}. \quad (\text{C16})$$

Appendix D: Limiting transitions

Below we demonstrate limiting transitions to the known cases of a plane wave and a Gaussian paraxial state. First we take the plane-wave limit of Eq. (46), which corresponds to $b_0 \rightarrow \infty$. Taking this limit, we find

$$\lim_{b_0 \rightarrow \infty} R(\theta, L, b_0) \propto \lim_{b_0 \rightarrow \infty} \frac{1}{b_0^8} = 0. \quad (\text{D1})$$

The Gaussian limit is recovered by setting $\ell^i = 0$, which immediately gives $d\dot{w}/d\theta = 0$.

Finally, in the limit $L \rightarrow \infty$ the rate scales as

$$\lim_{L \rightarrow \infty} \frac{d\dot{w}}{d\theta} \propto \lim_{L \rightarrow \infty} \frac{1}{L^2} = 0, \quad (\text{D2})$$

which highlights that the transition is a boundary (edge) effect.

[1] K. Bliokh, I. Ivanov, G. Guzzinati, L. Clark, R. Van Boxem, A. Béché, R. Juchtmans, M. Alonso, P. Schattschneider, F. Nori, and J. Verbeeck, *Physics Reports* **690**, 1 (2017).

[2] I. P. Ivanov, *Progress in Particle and Nuclear Physics* **127**, 103987 (2022).

[3] C. N. Alexeyev and M. A. Yavorsky, *Journal of Optics A: Pure and Applied Optics* **8**, 752 (2006).

[4] K. Y. Bliokh, *Phys. Rev. Lett.* **97**, 043901 (2006).

[5] K. Y. Bliokh, Y. P. Bliokh, S. Savel'ev, and F. Nori, *Phys. Rev. Lett.* **99**, 190404 (2007).

[6] P. Schattschneider, T. Schachinger, M. Stöger-Pollach, S. Löffler, A. Steiger-Thirsfeld, K. Bliokh, and F. Nori, *Nature communications* **5**, 4586 (2014).

[7] T. Schachinger, S. Löffler, M. Stöger-Pollach, and P. Schattschneider, *Ultramicroscopy* **158**, 17 (2015).

[8] Y. Wang, C. Jia, and P. Zhang, *Applied Physics Letters* **118**, 10.1063/5.0039479 (2021).

[9] D. Cozzolino, D. Bacco, B. Da Lio, K. Ingerslev, Y. Ding, K. Dalgaard, P. Kristensen, M. Galili, K. Rottwitt, S. Ramachandran, and L. K. Oxenløwe, *Phys. Rev. Appl.* **11**, 064058 (2019).

[10] T. Harvey, F. Venturi, J. Pierce, R. Balboni, F. Bouchard, G. C. Gazzadi, S. Frabboni, A. Tavabi, Z.-A. Li, R. Dunin-Borkowski, R. Boyd, B. McMorran, and E. Karimi, *Nature Communications* **8**, 10.1038/s41467-017-00829-5 (2017).

[11] V. A. Zaytsev, V. G. Serbo, and V. M. Shabaev, *Phys. Rev. A* **95**, 012702 (2017).

[12] Q. Meng, X. Liu, W. Ma, Z. Yang, L. Lu, A. J. Silenko, P. Zhang, and L. Zou, *Phys. Rev. Res.* **7**, 023306 (2025).

[13] I. P. Ivanov, N. Korchagin, A. Pimikov, and P. Zhang, *Phys. Rev. D* **101**, 016007 (2020).

[14] I. P. Ivanov, N. Korchagin, A. Pimikov, and P. Zhang, *Phys. Rev. D* **101**, 096010 (2020).

[15] L. Allen, M. Beijersbergen, R. Spreeuw, and J. Woerdman, *Physical review. A* **45**, 8185 (1992).

[16] D. Karlovets and A. Di Piazza, *Phys. Rev. D* **108**, 063007 (2023).

[17] L. L. Foldy and S. A. Wouthuysen, *Phys. Rev.* **78**, 29 (1950).

[18] H. R. Lewis, *Phys. Rev. Lett.* **18**, 510 (1967).

[19] H. R. Lewis, *Phys. Rev. Lett.* **18**, 636 (1967).

[20] H. R. Lewis and W. B. Riesenfeld, *J. Math. Phys.* **10**, 1458 (1969).

[21] V. Aldaya, F. Cossío, J. Guerrero, and F. F. López-Ruiz, *Journal of Physics A: Mathematical and Theoretical* **44**, 065302 (2011).

[22] F. López-Ruiz and J. Guerrero, *Journal of Physics Conference Series* **538**, 012015 (2014).

[23] A. Melkani and S. J. van Enk, *Phys. Rev. Res.* **3**, 033060 (2021).

[24] N. V. Filina and S. S. Baturin, *Phys. Rev. A* **108**, 012219 (2023).

[25] N. V. Filina and S. S. Baturin, *Phys. Rev. A* **110**, 022204 (2024).

[26] N. V. Filina and S. S. Baturin, *Phys. Rev. A* , (2026).

[27] Y. Aharonov and D. Bohm, *Physical Review* **115**, 485 (1959).

[28] H. J. Kimble, *Physica Scripta* **T76**, 127 (1998).

[29] P. A. M. Dirac and R. H. Fowler, *Proceedings of the Royal Society of London. Series A, Containing Papers of a Mathematical and Physical Character* **117**, 610 (1928).

[30] G. B. Folland, *Harmonic Analysis in Phase Space*, Annals of Mathematics Studies, Vol. 122 (Princeton University Press, Princeton, NJ, 1989).

[31] M. Fernández Guasti and H. M. Moya-Cessa, *Journal of Physics A: Mathematical and General* **36**, 2069 (2003).

[32] M. P. Morales Rodríguez, E. G. Herrera, O. S. Magaña Loaiza, B. Pérez-García, F. M. Gutiérrez, and B. M. Rodríguez-Lara, *Phys. Rev. A* **110**, 033523 (2024).

[33] A. A. Sokolov and I. M. Ternov, *Relativistic Electron* (Nauka, Moscow, 1974) p. 391, in Russian. Bibliography: pp. 380-385. Subject index: pp. 386-391.

[34] K. Saitoh, Y. Hasegawa, N. Tanaka, and M. Uchida, *Journal of Electron Microscopy* **61**, 171 (2012).

[35] J. Verbeeck, H. Tian, and P. Schattschneider, *Nature* **467**, 301 (2010).

[36] B. J. McMorran, A. Agrawal, I. M. Anderson, A. A. Herzing, H. J. Lezec, J. J. McClelland, and J. Unguris, *Science* **331**, 192 (2011).

[37] P. Schattschneider, T. Schachinger, M. Stöger-Pollach, S. Löffler, A. Steiger-Thirsfeld, K. Y. Bliokh, and F. Nori, *Nature Communications* **5**, 4586 (2014).

[38] A. H. Tavabi, P. Rosi, A. Roncaglia, E. Rotunno, M. Belleggia, P.-H. Lu, L. Belsito, G. Pozzi, S. Frabboni, P. Tiemeijer, R. E. Dunin-Borkowski, and V. Grillo, *Applied Physics Letters* **121**, 073506 (2022).

[39] E. M. Purcell, *Physical Review* **69**, 681 (1946).

[40] L. Zou, P. Zhang, and A. J. Silenko, *Phys. Rev. A* **103**, L010201 (2021).

[41] D. Karlovets, *New Journal of Physics* **23**, 033048 (2021).